Modeling interface-confined scalars and insoluble surfactants in two-phase flows

By S. S. Jain AND A. Mani

1. Motivation and objectives

The transport of scalars on evolving interfaces in fluids is a ubiquitous phenomenon across a broad range of processes in nature and in engineering, and is worthy of modeling. We, here, refer to an interface-confined scalar as any passive or active scalar quantity that is transported along an evolving/deforming interface. These scalars could represent charged species (Chu & Bazant 2007), surfactants (Hargreaves 2007), or any other conserved scalar quantity.

Surfactants lower the surface tension properties and generate Marangoni forces, which are useful in controlling the dynamics of multiphase flows. They are transported with the interface due to convection, diffuse along the interface when there is a concentration gradient, and can also be exchanged (adsorbed/desorbed) between the bulk and the interface (Defay *et al.* 1966). Surfactants have applications in industry in emulsification and mixing, drug delivery, droplet manipulation in microfluidics (Eggleton *et al.* 2001; Booty & Siegel 2005; Baret 2012; Pit *et al.* 2015), drag reduction (Manfield *et al.* 1999), and are important for the functioning of lungs (Yap & Gaver III 1998).

Research on modeling surfactants dates back to Stone (1990) and Wong *et al.* (1996). They derived a transport equation for the conservation of surfactants on evolving interfaces, given by

$$\frac{\partial \hat{c}}{\partial t} + \vec{u} \cdot \vec{\nabla} \hat{c} = \vec{\nabla}_s \cdot \left(D \vec{\nabla}_s \hat{c} \right) - \hat{c} \vec{\nabla}_s \cdot \vec{u}_s - \hat{c} \kappa \vec{u} \cdot \vec{n}, \tag{1.1}$$

where $\hat{c}$ is the interfacial scalar concentration (amount of scalar per unit area of the interface) and $\vec{\nabla}_s = (I - \vec{n} \otimes \vec{n}) \vec{\nabla}$ is the surface gradient. The effects of surfactants on drop/bubble deformation and breakup have been studied theoretically or semi-analytically by Stone & Leal (1990); Milliken *et al.* (1993); Milliken & Leal (1994); Pawar & Stebe (1996); Siegel (1999). One of the first coupled numerical simulations studying the effect of surfactants on the flow around bubbles was done by Cuenot *et al.* (1997). Since then, various methods have been proposed in the past for modeling insoluble surfactants. Using a boundary integral method, Li & Pozrikidis (1997); Yon & Pozrikidis (1998); Eggleton *et al.* (1999) studied the effect of insoluble surfactants on drops in Stokes flow, and Eggleton *et al.* (2001) simulated the tip streaming breakup of drops. A coupled grid-based particle method with an implicit boundary integral method was also proposed by Hsu *et al.* (2019).

In continuum approaches, and in the context of sharp-interface methods, insoluble surfactants have been modeled using a volume-of-fluid method by Renardy *et al.* (2002); Drumright-Clarke & Renardy (2004); James & Lowengrub (2004), using a Lagrangian-based finite-element formulation by Pozrikidis (2004); Ganesan & Tobiska (2009); Venkatesan *et al.* (2019); Frachon & Zahedi (2023), using a segment projection method by Khatri & Tornberg (2011), using a level-set method by Xu & Zhao (2003); Xu *et al.* (2006, 2012), using a front-tracking method with adaptive mesh refinement by de Jesus *et al.* (2015),

using an immersed-boundary method by Lai *et al.* (2008), and using hybrid methods by Ceniceros (2003); Cui (2011).

In the context of diffuse-interface methods, a free energy functional-based model has been used to model surfactants by Van der Sman & Van der Graaf (2006); Yun *et al.* (2014), and the well-posedness of the system has been studied by Engblom *et al.* (2013); Abels *et al.* (2019); Di Primio *et al.* (2022). All the methods use a Cahn-Hilliard-based diffuse-interface framework for modeling surfactants (Teigen *et al.* 2009, 2011; Garcke *et al.* 2014; Ray *et al.* 2021). More recently, the effects of surfactants on breakup and coalescence of droplets in a turbulent flow, was studied by Soligo *et al.* (2019), along with their feedback effect on the flow by Soligo *et al.* (2020). However, to the best of our knowledge, there is no model for transport of surfactants or interface-confined scalars for second-order phase-field methods.

We recently developed a model for transport of scalars in the bulk in Jain & Mani (2023), given by

$$\frac{\partial c}{\partial t} + \vec{\nabla} \cdot (\vec{u}c) = \vec{\nabla} \cdot \left[D \left\{ \vec{\nabla} c - \frac{(1-\phi)\vec{n}c}{\epsilon} \right\} \right], \tag{1.2}$$

where c is the scalar concentration (amount of scalar per unit volume), and showed that the model results in the consistent transport of scalar with the phase-field variable and will not result in artificial leakage of scalar across the interface. This model was also extended to include transfer across the interface by Mirjalili *et al.* (2022).

The primary objective of the present work is to propose a computational model for transport of scalars that are confined to material interfaces. In this work, we propose a consistent method that results in leakage-proof transport of scalars along the convecting and deforming material interface. We prove and show that the scalar remains positive, which is a physical-realizability condition, using second-order central-difference schemes.

We use a second-order phase-field method, particularly the accurate conservative phase-field/diffuse-interface (ACDI) method by Jain (2022), for modeling the interface in a two-phase flow. The proposed model in this work can also be used with a conservative phase-field/diffuse-interface (CDI) method (Chiu & Lin 2011), a conservative level-set (CLS) method (Olsson & Kreiss 2005), an accurate conservative level-set (ACLS) method (Desjardins *et al.* 2008), including compressible diffuse-interface methods (Jain *et al.* 2020, 2021), and any other method that results in a hyperbolic tangent interface shape in equilibrium, and when the volume fraction ϕ is bounded between 0 and 1. For coupling with other models, like a Cahn-Hilliard model where the volume fraction takes values between -1 and 1, the proposed model can be affine transformed with respect to the order parameter, such that the change in the range from $[0, 1]$ to the range of values of ϕ that the interface-capturing model admits is accounted for.

We present one-way coupled simulations of transport of scalars confined to the interface to illustrate the accuracy, consistency, and robustness of the proposed method in localizing the scalar to the interface location and in maintaining the leak-proof condition. The two-way coupled (coupling back with hydrodynamics) simulations are deferred to a future work.

2. Phase-field model

In this work, we use the recently developed accurate conservative phase-field/diffuse-interface model (ACDI) by Jain (2022), which is an Allen-Cahn-based second-order

phase-field model given by

$$\frac{\partial \phi}{\partial t} + \vec{\nabla} \cdot (\vec{u}\phi) = \vec{\nabla} \cdot \left\{ \Gamma \left\{ \epsilon \vec{\nabla}\phi - \frac{1}{4} \left[1 - \tanh^2 \left(\frac{\psi}{2\epsilon} \right) \right] \frac{\vec{\nabla}\psi}{|\vec{\nabla}\psi|} \right\} \right\}, \tag{2.1}$$

where ϕ is the phase-field variable that represents the volume fraction, $\vec{u}$ is the velocity, Γ represents the velocity-scale parameter, ϵ is the interface thickness scale parameter, and ψ is an auxiliary signed-distance-like variable given by

$$\psi = \epsilon \ln \left(\frac{\phi + \varepsilon}{1 - \phi + \varepsilon} \right), \tag{2.2}$$

where $\varepsilon = 10^{-100}$ is a small number. The parameters are chosen to be $\Gamma \geq |\vec{u}|_{max}$ and $\epsilon > 0.5\Delta x$, along with Δt satisfying the explicit Courant-Friedrich-Lewy criterion, to maintain the boundedness of ϕ (Jain 2022).

The ACDI model is known to be more accurate than other phase-field models because it maintains a sharper interface (with only one-to-two grid points across the interface) while being robust and conservative, without the need for any geometric treatment.

3. Proposed model for the transport of scalars/surfactants on evolving interfaces

The proposed model for the transport of interface-confined scalars and insoluble surfactants on an evolving interfaces is

$$\frac{\partial c}{\partial t} + \vec{\nabla} \cdot (\vec{u}c) = \vec{\nabla} \cdot \left[D \left\{ \vec{\nabla}c - \frac{2(0.5 - \phi)\vec{n}c}{\epsilon} \right\} \right], \tag{3.1}$$

where D is the diffusivity of the scalar, and $\vec{n} = \vec{\nabla}\phi/|\vec{\nabla}\phi| = \vec{\nabla}\psi/|\vec{\nabla}\psi|$ is the interface normal vector. The second term on the right-hand side (RHS) of Eq. (3.1) is an artificial sharpening term. The effect of this sharpening flux is to prevent the diffusion of the scalar on both sides of the interface and to confine it to the interface region, which is illustrated in Figure 1.

Note the similarity of this sharpening flux to the model for transport of scalars in the bulk in Eq. (1.2), where the scalar is confined to one of the phases. The difference between the proposed model in Eq. (3.1) and the one in Eq. (1.2) is the sharpening flux. The sharpening flux in Eq. (1.2) acts along one direction and prevents the leakage of the scalar from one of the phases into the other phase, whereas in Eq. (3.1), the sharpening flux acts in both directions, preventing the scalar from diffusing away from the interface region into either of the phases on both sides of the interface.

3.1. *Consistency and equilibrium solution*

It is well known that the equilibrium solution (when $\Gamma \to \infty$) for the phase-field model in Eq. (2.1) is a hyperbolic tangent function given by

$$\phi_{eq} = \frac{1}{2} \left[1 + \tanh \left(\frac{x}{2\epsilon} \right) \right] \sim \tanh \left(\frac{x}{2\epsilon} \right). \tag{3.2}$$

Now, taking a derivative of the equilibrium solution, we obtain

$$\phi'_{eq} \sim \frac{1}{4\epsilon \cosh^2 \left(\frac{x}{2\epsilon} \right)}. \tag{3.3}$$

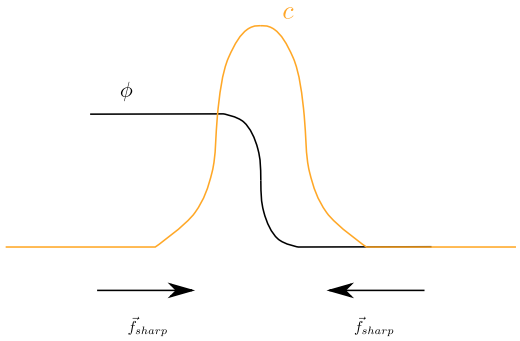

FIGURE 1. Schematic representing the effect of sharpening flux $\vec{f}_{sharp} = D2(0.5-\phi)\vec{n}c/\epsilon$ in the model. Here, ϕ and c are plotted at equilibrium to illustrate their equilibrium solutions: $\phi \sim \phi_{eq}$ and $c \sim \phi'_{eq}$.

This function is analogous to a Dirac delta function, a derivative of a step function, for the hyperbolic tangent function. Hence, a consistent transport model for interface-confined scalars and insoluble surfactants should possess an equilibrium solution of the form in Eq. (3.3). Both ϕ_{eq} and ϕ'_{eq} are shown in Figure 1.

To verify the equilibrium solution for the proposed model in Eq. (3.1), let's assume steady state, and $\vec{u} = 0$. In one dimension, the proposed model reduces to the form

$$0 = \vec{\nabla} \cdot \left[D \left\{ \vec{\nabla} c - \frac{2(0.5-\phi)\vec{n}c}{\epsilon} \right\} \right] \Rightarrow \frac{d^2c}{dx^2} - \frac{1}{\epsilon}\frac{d\left\{2(0.5-\phi)c\right\}}{dx} = 0 \tag{3.4}$$

for $\vec{n} = +1$. Assuming the interface is at the origin and is in equilibrium, then

$$\phi = \phi_{eq} = \frac{e^{(x/\epsilon)}}{1+e^{(x/\epsilon)}} = \frac{1}{2}\left\{1 + \tanh\left(\frac{x}{2\epsilon}\right)\right\}. \tag{3.5}$$

Using Eq. (3.5) and solving for c by integrating the Eq. (3.4) and using the boundary conditions

$$c = \begin{cases} 0 & x \to -\infty \\ c_0 & x = 0, \end{cases} \quad \text{and} \quad \frac{dc}{dx} \to 0 \quad \text{for} \quad x \to -\infty, \tag{3.6}$$

we obtain

$$c = \frac{c_0}{\cosh^2\left(\frac{x}{2\epsilon}\right)}. \tag{3.7}$$

Therefore, the equilibrium kernel function for the proposed model in Eq. (3.1) is $c_{eq} \sim \phi'_{eq}$ [Eq. (3.3)]. Hence, the model is consistent with the phase-field model. This results in the transport of the scalar along the interface without any unphysical numerical leakage into either of the phases on the two sides of the interface.

3.2. *Generalized model*

The proposed model in Eq. (3.1) can be generalized as

$$\frac{\partial c}{\partial t} + \vec{\nabla} \cdot (\vec{u}c) = \vec{\nabla} \cdot \left[D \left\{ \vec{\nabla} c - \frac{a(0.5-\phi)\vec{n}c}{\epsilon} \right\} \right], \tag{3.8}$$

where a is a constant. Theoretically, any value for a is valid, provided the positivity is maintained (see, Section 6.1.2), and a higher value for a results in sharper representation of the scalar at the interface, which is illustrated in Section 6.1.3. However, note the model

is only exactly consistent with the phase-field model for $a = 2$, which is the recommended value.

3.3. *Two-way coupling and soluble surfactants*

Some surfactants are also soluble in the bulk phase. Some are soluble in both bulk phases and some are soluble in only one of the bulk phases, but for either case, the proposed model in this work can be coupled with the scalar transport model in Jain & Mani (2023), which will account for the transport of the scalar in the bulk phase. This coupling between surface and bulk phases can be incorporated using source/sink terms. Furthermore, to account for two-way coupling with hydrodynamics, a Langmuir equation of state or a linearized version of this equation of state can be used. Both two-way coupling and soluble surfactants are deferred to future work.

3.4. *Relationship with the sharp-interface surfactant-transport models*

The sharp-interface model in Eq. (1.1) can be rewritten in a distribution form (Teigen *et al.* 2009) as

$$\frac{\partial\left(\hat{c}\delta_s\right)}{\partial t} + \vec{\nabla}\cdot\left(\vec{u}\hat{c}\delta_s\right) = \vec{\nabla}\cdot\left(D\delta_s\vec{\nabla}\hat{c}\right), \tag{3.9}$$

where δ_s is a surface delta function, defined as

$$\int_\gamma \hat{c}d\gamma = \int_\Omega \hat{c}\delta_s d\omega, \tag{3.10}$$

where γ is the interface and Ω is the domain. The model in Eq. (3.9) can be solved directly by assuming a form for the surface delta function, an approach that was taken by Teigen *et al.* (2009). They used $\delta_s = 3\sqrt{2}\phi^2(1-\phi)^2/\epsilon$ and solved Eq. (3.9) with a Cahn-Hilliard phase-field model. However, this approach requires dividing $\hat{c}\delta_s$ by δ_s to compute $\hat{c}$ in the diffusion term in Eq. (3.9), which could result in robustness issues.

The proposed model in Eq. (3.1) can be derived starting from the transport equation in Eq. (3.9) by relating c and $\hat{c}$ as

$$\hat{c} = \frac{c}{\delta_s}. \tag{3.11}$$

Using this relation in Eq. (3.9),

$$\frac{\partial c}{\partial t} + \vec{\nabla}\cdot\left(\vec{u}c\right) = \vec{\nabla}\cdot\left[D\left\{\vec{\nabla}c - \frac{c}{\delta_s}\vec{\nabla}\delta_s\right\}\right], \tag{3.12}$$

invoking equilibrium

$$\vec{\nabla}\phi = \frac{\phi(1-\phi)}{\epsilon}\vec{n}, \tag{3.13}$$

and assuming the form for the surface delta function to be

$$\delta_s = |\vec{\nabla}\phi|, \tag{3.14}$$

we arrive at

$$\frac{\partial c}{\partial t} + \vec{\nabla}\cdot\left(\vec{u}c\right) = \vec{\nabla}\cdot\left[D\left\{\vec{\nabla}c - \frac{2(0.5-\phi)c}{\epsilon}\frac{\vec{\nabla}\phi}{|\vec{\nabla}\phi|}\right\}\right], \tag{3.15}$$

which is the proposed model in Eq. (3.1) if $\vec{n} = \vec{\nabla}\phi/|\vec{\nabla}\phi|$. Note that it is not required to perform division by δ_s anywhere in the proposed model, which makes the method robust. Moreover, the surface gradient operator $\vec{\nabla}_s$ is not used in the proposed model. Modeling

such gradients accurately and efficiently requires infrastructure that is not needed with the proposed model, making it robust and easy to implement.

4. Positivity

Following the proof of positivity in Jain & Mani (2023), the interfacial scalar or surfactant concentration c in Eq. (3.1) can be shown to remain positive, i.e., $c_i^k \geq 0 \; \forall k \in \mathbb{Z}^+$, where k is the time-step index and i is the grid index, provided the constraints

$$\Delta x \leq \left(\frac{2D}{|u|_{\max} + \frac{Da}{2\epsilon}} \right), \tag{4.1}$$

and

$$\Delta t \leq \frac{\Delta x^2}{2N_d D} \tag{4.2}$$

are satisfied, where Δx is the grid-cell size, Δt is the time-step size, $|u|_{\max}$ is the maximum fluid velocity in the domain, and N_d is the number of dimensions. Note that this also requires ϕ_i^k to be bounded between 0 and 1, $\forall k \in \mathbb{Z}^+$ and $\forall i$, which is guaranteed to be satisfied with the ACDI method (Jain 2022).

If $\epsilon = \Delta x$, then the positivity constraint in Eq. (4.1) reduces to $\Delta x \leq D(2 - a/2)/|u|_{\max}$. Hence, positivity can be achieved as long as $a < 4$. If $a = 2$, then the constraint is

$$\Delta x \leq \frac{D}{|u|_{\max}} \text{ or } Pe_c \leq 1, \tag{4.3}$$

where $Pe_c = \Delta x |u|_{\max}/D$ is the cell-Peclet number. Similarly, for $\epsilon = 0.75\Delta x$ and $a = 2$, the constraint is $Pe_c \leq 0.67$, and for $\epsilon = 0.6\Delta x$ and $a = 2$, the constraint is $Pe_c \leq 0.33$.

5. Numerical methods

In this work, we use a second-order central scheme for spatial discretization and a fourth-order Runge-Kutta scheme for time stepping for the proposed model in Eq. (3.1). A skew-symmetric-like flux-splitting approach (Jain & Moin 2022) is adopted for the discretization of the ACDI method in Eq. (2.1).

6. Simulation results

In this section, simulations of the proposed model coupled with the ACDI method are presented. The simulations can be subdivided into four categories: (a) verification of the confinement of the scalar to the interface region in Section 6.1.1, (b) verification of the positivity of the scalar in Section 6.1.2, (c) effect of the choice of constant coefficient a in the generalized version of the model in Section 6.1.3, and (d) multidimensional simulations which include a moving drop with an initially uniform scalar distribution, an extension of the one-dimensional cases, as well as a stationary drop with a nonuniform scalar distribution along the interface in Section 6.2.

6.1. *One-dimensional simulations*

In this section, one-dimensional simulations are presented, which act as verification of the proposed model. In all the simulations, a unit domain length of $L = 1$ is used with a grid size of $\Delta x = 0.01$, unless specified otherwise. A drop of radius $R = 0.2$ is initially

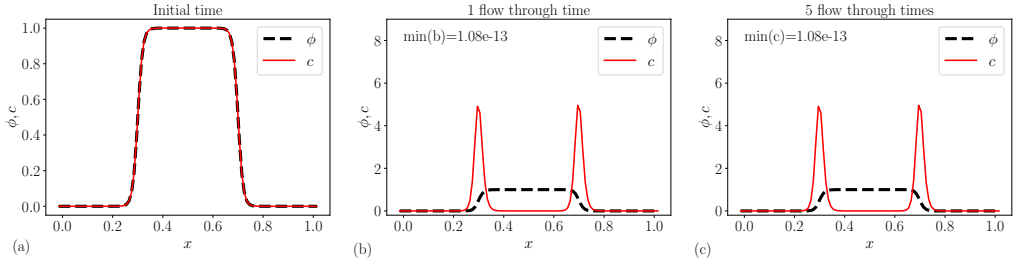

FIGURE 2. The advection of a drop along with an initially uniformly distributed scalar quantity (dissolved scalar in the bulk) inside the drop. (a) The initial drop and scalar setup, (b) the drop and scalar after 1 flow-through time at $t = 2$, and (c) the drop and scalar after 5 flow-through times at $t = 10$.

placed in the domain centered at $x_c = 0.5$. The initial condition for the drop is given by $\phi_i = 0.5\,[1 - \tanh\{(|x - 0.5| - 0.2)/(2\epsilon)\}]$, where the subscript i denotes $t = 0$.

6.1.1. *Confinement verification*

To verify the effectiveness of the artificial sharpening term in the proposed model in Eq. (3.1) to confine the scalar to the interface region, we initialize the scalar uniformly within the drop in this section with a concentration of unity ($c_i = \phi_i$). Since the scalar is not permitted to dissolve into the bulk phase, we expect it to get reorganized and move to the interface region.

For the simulations in this section, a uniform velocity of $\vec{u} = 0.5$ is prescribed, and both the drop and the scalar are advecting with this velocity field. The drop and the scalar are advected with a nonzero velocity field to verify the ability of the proposed model to reorganize the scalar field relative to the background flow field. The diffusivity is chosen to be $D = 0.01$, so the $Pe_c = 0.5$.

Figure 2 shows the evolution of the scalar with time. After 1 flow-through time, the scalar has reorganized to the interface region and has reached a steady state. After 5 flow-through times, the scalar is still confined to the interface region, as both the scalar and the drop are advecting with a velocity of $\vec{u} = 0.5$.

The artificial sharpening flux in Eq. (3.1) is responsible for the reorganization of the scalar. Therefore, the velocity associated with this reorganization of the scalar is given by $\vec{u}_{re\_org} \approx D2(0.5 - \phi)\vec{n}/\epsilon$. For the parameters chosen in this section, $\vec{u}_{re\_org} \approx 1$. Therefore, $\vec{u}_{re\_org}$ is larger than the advection velocity $\vec{u}$, and this is the case as long as the positivity criterion in Eq. (4.3) is satisfied. Hence, the sharpening flux will always dominate over any other background flow, thus resulting in the confinement of the scalar to the interface region.

6.1.2. *Positivity verification*

In this section, the robustness of the positivity criterion in Eqs. (4.1) and (4.3) is evaluated. The setup used here is the same as the one in Section 6.1.1. But two different diffusivities are chosen, $D = 0.01$ and $D = 0.0025$, which will result in $Pe_c = 0.5$ and $Pe_c = 2$, respectively. Since the simulation with $D = 0.0025$ does not satisfy the positivity criterion, we expect the scalar to violate the positivity.

Figure 3 shows the final state of the drop and the scalar after 1 flow-through time. The minimum value of the scalar concentration field seen is also reported in the plots. As expected, the simulation with $Pe_c = 2$ violates the positivity criterion, and therefore, negative values of the scalar concentration are observed.

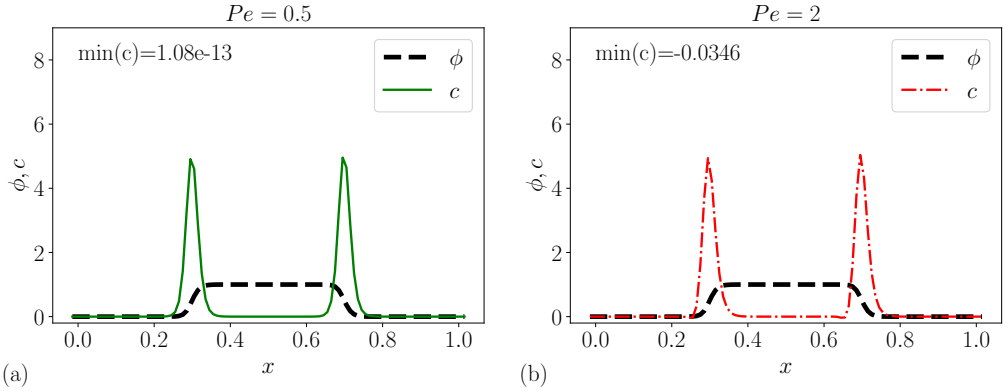

FIGURE 3. Final state of the drop and the scalar concentration field at time $t = 2$. The two plots represent the two diffusivities chosen to test the positivity of the scalar: (a) $Pe_c = 0.5$ and (b) $Pe_c = 2$.

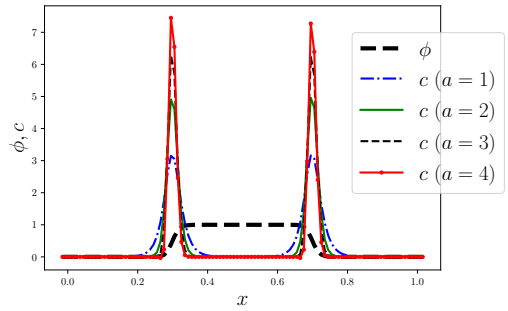

FIGURE 4. Final state of the drop and the scalar concentration field at time $t = 2$ with various values of a in Eq. (3.8).

6.1.3. *Effect of* a

In this section, the effect of using a value other than $a = 2$ in the generalized model in Eq. (3.8) is illustrated. The setup is the same as the one in Section 6.1.1 with $Pe_c = 0.5$, and four different values $a = 1, 2, 3$, and 4 are tested. Figure 4 shows the final state of the drop and the scalar after 1 flow-through time. The positivity of the scalar was verified for the cases $a = 1, 2$, and 3, and the positivity was violated for $a = 4$ as expected (see Section 4).

With the increase in a, the scalar is more concentrated at the interface. This might result in an improved accuracy due to a sharper representation of the interface-confined scalar. However, note that only the value of $a = 2$ will result in a model that is exactly consistent with the phase-field model, as described in Section 3.2, and therefore $a = 2$ is the recommended value.

6.2. *Multidimensional simulations*

In this section, the applicability of the proposed model for simulating multidimensional problems is tested. Two simulation setups in the subsequent sections are chosen: (a) Advecting drop—a two-dimensional version of the simulations in Section 6.1.1, and (b) surface diffusion of the scalar—a verification case, where the relative diffusion of the scalar along the interface is tested and compared against the analytical solutions.

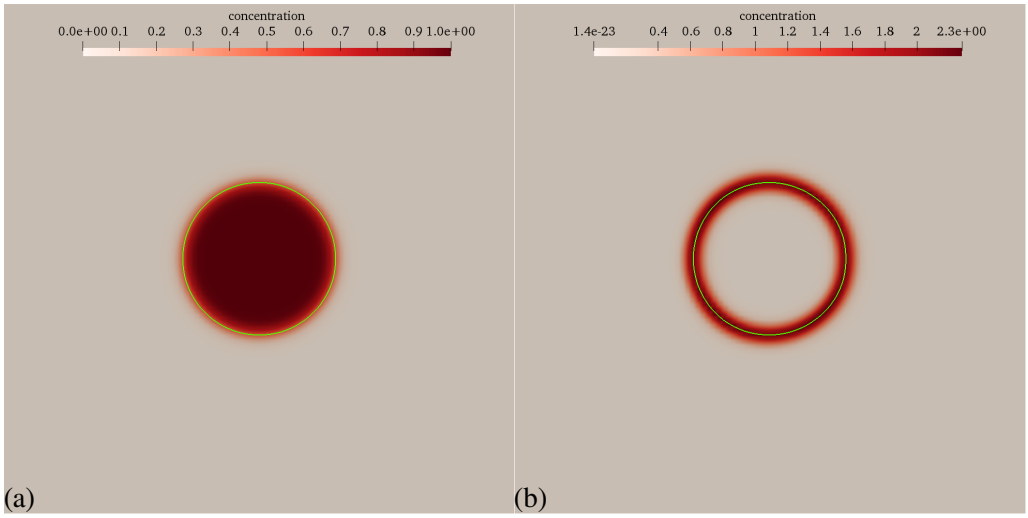

FIGURE 5. The advection of a two-dimensional drop along with an initially uniformly distributed scalar quantity (dissolved scalar in the bulk) inside the drop. (a) The drop and scalar setup at initial time. (b) The drop and scalar after 1 flow-through time at $t = 2$. The solid green line is the isocontour of $\phi = 0.5$ which represents the interface.

6.2.1. *Advecting drop*

In this simulation, a unit square domain of size $L = 1\times1$ is used with a grid size of $\Delta x = 0.01$. A drop of radius $R = 0.2$ is initially placed in the domain center $(0.5, 0.5)$. The initial condition for the drop is given by $\phi_i = 0.5\left[1 - \tanh\left\{\left((x-0.5)^2 + (y-0.5)^2 - 0.2\right)/(2\epsilon)\right\}\right]$. The scalar is initialized uniformly within the drop ($c_i = \phi_i$). A uniform velocity of $\vec{u} = 0.5$ is prescribed, and $Pe_c = 0.5$. As was seen in Section 6.1.1 for the one-dimensional setup, we expect the scalar to reorganize and move to the interface region.

Figure 5 shows the scalar concentration and the drop at the initial and final time of $t = 2$. As expected, the scalar reorganizes and moves to the interface region, since it is not allowed to dissolve in the bulk phase. This verifies the applicability of the proposed model in Eq. (3.1) in multidimensional problems without difficulty.

6.2.2. *Surface diffusion of scalar*

In this section, the scalar is initially confined to the interface of a stationary drop, but with a non-uniform concentration profile along the interface. The diffusion of the scalar along the interface is verified by comparing against analytical solutions.

The initial interfacial concentration (concentration per unit area of the interface) of the scalar is chosen to be

$$\hat{c}(\theta) = \frac{1}{2}\{1 - \cos\theta\}. \tag{6.1}$$

By solving a surface concentration equation in polar coordinates, the analytical solution for the diffusion of the scalar along the circular interface can be derived as

$$\hat{c}(\theta, t) = \frac{1}{2}\left(1 - e^{-\frac{D}{R^2}t}\cos\theta\right). \tag{6.2}$$

The simulation domain is chosen to be $[-2, 2] \times [-2, 2]$, with a grid size of 100×100, and the drop radius is $R = 1$. Figure 6 shows the scalar concentration at the initial and final time of $t = 1$, which illustrates the diffusion of the scalar along the interface

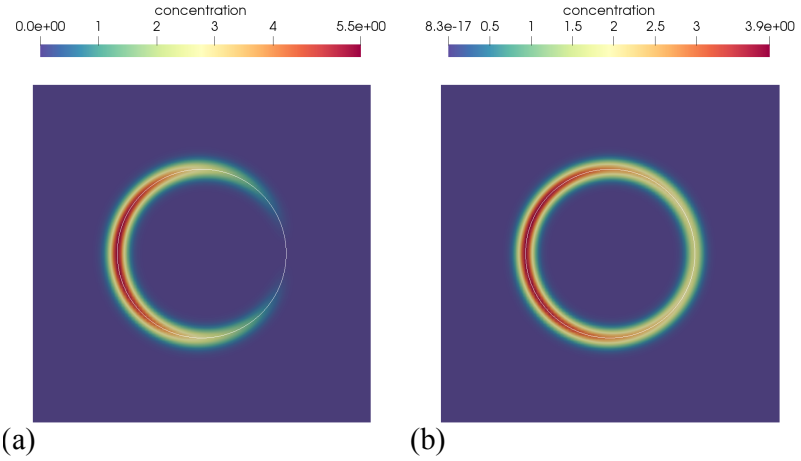

FIGURE 6. The surface diffusion of scalar on a two-dimensional stationary drop. (a) The drop and scalar setup at initial time. (b) The drop and scalar configuration at $t = 1$.

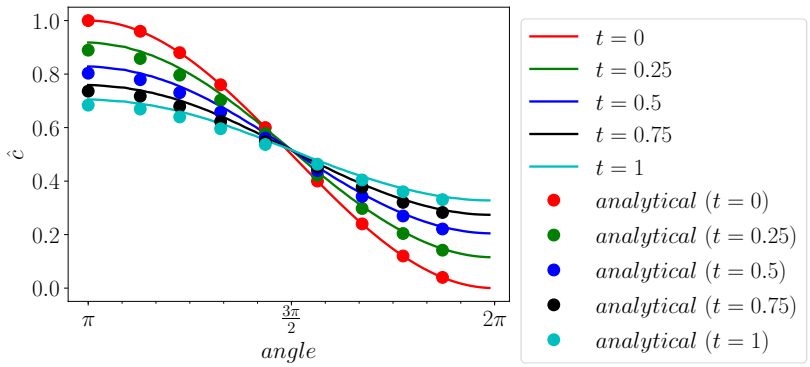

FIGURE 7. The local interfacial concentration of the scalar $\hat{c}$ along the drop at various time instances, computed using the proposed method, and its comparison with the analytical solution in Eq. (6.2).

without any artificial leakage into the bulk phases. A quantitative comparison of the scalar concentration is shown in Figure 7 at various times, verifying the proposed model's capability to accurately simulate the transport of scalars that are confined to evolving material interfaces.

7. Conclusion

In this work, a model for the transport of scalars confined to evolving material interfaces and insoluble surfactants in two-phase flows is developed. The model is solved with a second-order phase-field model; however, it also can be used with other interface-capturing methods. The scalar is shown to be consistently transported with the phase-field variable, resulting in a method that does not allow artificial leakage of the scalar into the bulk phases on either side of the interface. The model also results in positive scalar concentrations, a physical-realizability condition, provided the given positivity criterion is satisfied.

The proposed model was used to simulate transport of scalars on interfaces in a wide range of one-dimensional and two-dimensional settings. The model was verified in terms of its capability to enforce confinement of the scalar to the interface region, the positivity of the scalar concentration, and its applicability for multidimensional problems. The accuracy of the model was also verified by comparing against analytical solutions.

Acknowledgments

S. S. J. acknowledges financial support from Boeing Co.

REFERENCES

Abels, H., Garcke, H. & Weber, J. 2019 Existence of weak solutions for a diffuse interface model for two-phase flow with surfactants. *Commun. Pure Appl. Anal.* **18**, 195.

Baret, J.-C. 2012 Surfactants in droplet-based microfluidics. *Lab Chip* **12**, 422–433.

Booty, M. & Siegel, M. 2005 Steady deformation and tip-streaming of a slender bubble with surfactant in an extensional flow. *J. Fluid Mech.* **544**, 243–275.

Ceniceros, H. D. 2003 The effects of surfactants on the formation and evolution of capillary waves. *Phys. Fluids* **15**, 245–256.

Chiu, P.-H. & Lin, Y.-T. 2011 A conservative phase field method for solving incompressible two-phase flows. *J. Comput. Phys.* **230**, 185–204.

Chu, K. T. & Bazant, M. Z. 2007 Surface conservation laws at microscopically diffuse interfaces. *J. Colloid Interface Sci.* **315**, 319–329.

Cuenot, B., Magnaudet, J. & Spennato, B. 1997 The effects of slightly soluble surfactants on the flow around a spherical bubble. *J. Fluid Mech.* **339**, 25–53.

Cui, Y. 2011 *A Computational Fluid Dynamics Study of Two-Phase Flows in the Presence of Surfactants*. University of New Hampshire.

de Jesus, W. C., Roma, A. M., Pivello, M. R., Villar, M. M. & da Silveira-Neto, A. 2015 A 3D front-tracking approach for simulation of a two-phase fluid with insoluble surfactant. *J. Comput. Phys.* **281**, 403–420.

Defay, R., Prigogine, I. & Bellemans, A. 1966 *Surface Tension and Adsorption*. Wiley.

Desjardins, O., Moureau, V. & Pitsch, H. 2008 An accurate conservative level set/ghost fluid method for simulating turbulent atomization. *J. Comput. Phys.* **227**, 8395–8416.

Di Primio, A., Grasselli, M. & Wu, H. 2022 Well-posedness for a Navier-Stokes-Cahn-Hilliard system for incompressible two-phase flows with surfactant. arXiv:2201.09022.

Drumright-Clarke, M. & Renardy, Y. 2004 The effect of insoluble surfactant at dilute concentration on drop breakup under shear with inertia. *Phys. Fluids* **16**, 14–21.

Eggleton, C. D., Pawar, Y. P. & Stebe, K. J. 1999 Insoluble surfactants on a drop in an extensional flow: a generalization of the stagnated surface limit to deforming interfaces. *J. Fluid Mech.* **385**, 79–99.

Eggleton, C. D., Tsai, T.-M. & Stebe, K. J. 2001 Tip streaming from a drop in the presence of surfactants. *Phys. Rev. Lett.* **87**, 048302.

Engblom, S., Do-Quang, M., Amberg, G. & Tornberg, A.-K. 2013 On diffuse interface modeling and simulation of surfactants in two-phase fluid flow. *Commun. Comput. Phys.* **14**, 879–915.

Frachon, T. & Zahedi, S. 2023 A cut finite element method for two-phase flows with insoluble surfactants. *J. Comput. Phys.* **473**, 111734.

Ganesan, S. & Tobiska, L. 2009 A coupled arbitrary Lagrangian–Eulerian and Lagrangian method for computation of free surface flows with insoluble surfactants. *J. Comput. Phys.* **228**, 2859–2873.

Garcke, H., Lam, K. F. & Stinner, B. 2014 Diffuse interface modelling of soluble surfactants in two-phase flow. *Commun. Math. Sci.* **12**, 1475–1522.

Hargreaves, A. E. 2007 Chemical Formulation: An Overview of Surfactant-Based Chemical Preparations Used in Everyday Life. Royal Society of Chemistry.

Hsu, S.-H., Chu, J., Lai, M.-C. & Tsai, R. 2019 A coupled grid based particle and implicit boundary integral method for two-phase flows with insoluble surfactant. *J. Comput. Phys.* **395**, 747–764.

Jain, S. S. 2022 Accurate conservative phase-field method for simulation of two-phase flows. *J. Comput. Phys.* **469**, 111529.

Jain, S. S., Adler, M. C., West, J. R., Mani, A., Moin, P. & Lele, S. K. 2021 Assessment of diffuse-interface methods for compressible multiphase fluid flows and elastic-plastic deformation in solids. arXiv:2109.09729 .

Jain, S. S. & Mani, A. 2023 A computational model for transport of immiscible scalars in two-phase flows. *J. Comput. Phys. (in press)* **475**.

Jain, S. S., Mani, A. & Moin, P. 2020 A conservative diffuse-interface method for compressible two-phase flows. *J. Comput. Phys.* **418**, 109606.

Jain, S. S. & Moin, P. 2022 A kinetic energy–and entropy-preserving scheme for compressible two-phase flows. *J. Comput. Phys.* **464**, 111307.

James, A. J. & Lowengrub, J. 2004 A surfactant-conserving volume-of-fluid method for interfacial flows with insoluble surfactant. *J. Comput. Phys.* **201**, 685–722.

Khatri, S. & Tornberg, A.-K. 2011 A numerical method for two phase flows with insoluble surfactants. *Comput. Fluids* **49**, 150–165.

Lai, M.-C., Tseng, Y.-H. & Huang, H. 2008 An immersed boundary method for interfacial flows with insoluble surfactant. *J. Comput. Phys.* **227** (15), 7279–7293.

Li, X. & Pozrikidis, C. 1997 The effect of surfactants on drop deformation and on the rheology of dilute emulsions in Stokes flow. *J. Fluid Mech.* **341**, 165–194.

Manfield, P., Lawrence, C. & Hewitt, G. F. 1999 Drag reduction with additives in multiphase flow: a literature survey. *Multiph. Sci. Tech.* **11**, 197–221.

Milliken, W. J. & Leal, L. G. 1994 The influence of surfactant on the deformation and breakup of a viscous drop: The effect of surfactant solubility. *J. Colloid Interface Sci.* **166** (2), 275–285.

Milliken, W. J., Stone, H. A. & Leal, L. 1993 The effect of surfactant on the transient motion of Newtonian drops. *Phys. Fluids A: Fluid Dyn.* **5**, 69–79.

Mirjalili, S., Jain, S. S. & Mani, A. 2022 A computational model for interfacial heat and mass transfer in two-phase flows using a phase field method. *Int. J. Heat Mass Transf.* **197**, 123326.

Olsson, E. & Kreiss, G. 2005 A conservative level set method for two phase flow. *J. Comput. Phys.* **210**, 225–246.

Pawar, Y. & Stebe, K. J. 1996 Marangoni effects on drop deformation in an exten-

sional flow: The role of surfactant physical chemistry. I. insoluble surfactants. *Phys. Fluids* **8**, 1738–1751.

Pit, A. M., Duits, M. H. & Mugele, F. 2015 Droplet manipulations in two phase flow microfluidics. *Micromachines* **6**, 1768–1793.

Pozrikidis, C. 2004 A finite-element method for interfacial surfactant transport, with application to the flow-induced deformation of a viscous drop. *J. Eng. Math.* **49**, 163–180.

Ray, D., Liu, C. & Riviere, B. 2021 A discontinuous Galerkin method for a diffuse-interface model of immiscible two-phase flows with soluble surfactant. *Comput. Geosci.* **25**, 1775–1792.

Renardy, Y. Y., Renardy, M. & Cristini, V. 2002 A new volume-of-fluid formulation for surfactants and simulations of drop deformation under shear at a low viscosity ratio. *Eur. J. Mech. B Fluids* **21**, 49–59.

Siegel, M. 1999 Influence of surfactant on rounded and pointed bubbles in two-dimensional stokes flow. *SIAM J. Appl. Math.* **59**, 1998–2027.

Van der Sman, R. & Van der Graaf, S. 2006 Diffuse interface model of surfactant adsorption onto flat and droplet interfaces. *Rheol. Acta* **46**, 3–11.

Soligo, G., Roccon, A. & Soldati, A. 2019 Breakage, coalescence and size distribution of surfactant-laden droplets in turbulent flow. *J. Fluid Mech.* **881**, 244–282.

Soligo, G., Roccon, A. & Soldati, A. 2020 Effect of surfactant-laden droplets on turbulent flow topology. *Phys. Rev. Fluids* **5**, 073606.

Stone, H. 1990 A simple derivation of the time-dependent convective-diffusion equation for surfactant transport along a deforming interface. *Phys. Fluids A Fluid Dyn.* **2**, 111–112.

Stone, H. A. & Leal, L. G. 1990 The effects of surfactants on drop deformation and breakup. *J. Fluid Mech.* **220**, 161–186.

Teigen, K. E., Li, X., Lowengrub, J., Wang, F. & Voigt, A. 2009 A diffuse-interface approach for modeling transport, diffusion and adsorption/desorption of material quantities on a deformable interface. *Commun. Math. Sci.* **4**, 1009.

Teigen, K. E., Song, P., Lowengrub, J. & Voigt, A. 2011 A diffuse-interface method for two-phase flows with soluble surfactants. *J. Comput. Phys.* **230**, 375–393.

Venkatesan, J., Padmanabhan, A. & Ganesan, S. 2019 Simulation of viscoelastic two-phase flows with insoluble surfactants. *J. Non-Newton. Fluid Mech.* **267**, 61–77.

Wong, H., Rumschitzki, D. & Maldarelli, C. 1996 On the surfactant mass balance at a deforming fluid interface. *Phys. Fluids* **8**, 3203–3204.

Xu, J.-J., Li, Z., Lowengrub, J. & Zhao, H. 2006 A level-set method for interfacial flows with surfactant. *J. Comput. Phys.* **212**, 590–616.

Xu, J.-J., Yang, Y. & Lowengrub, J. 2012 A level-set continuum method for two-phase flows with insoluble surfactant. *J. Comput. Phys.* **231**, 5897–5909.

Xu, J.-J. & Zhao, H.-K. 2003 An eulerian formulation for solving partial differential equations along a moving interface. *J. Sci. Comput.* **19**, 573–594.

Yap, D. Y. & Gaver III, D. P. 1998 The influence of surfactant on two-phase flow in a flexible-walled channel under bulk equilibrium conditions. *Phys. Fluids* **10**, 1846–1863.

Yon, S. & Pozrikidis, C. 1998 A finite-volume/boundary-element method for flow

past interfaces in the presence of surfactants, with application to shear flow past a viscous drop. *Comput. Fluids* **27**, 879–902.

Yun, A., Li, Y. & Kim, J. 2014 A new phase-field model for a water–oil-surfactant system. *Appl. Math. Comput.* **229**, 422–432.